Published in final edited form as:
Circ Res. 2014 June 20; 115(1): 68–78. doi:10.1161/CIRCRESAHA.115.304149.

EHD3-Dependent Endosome Pathway Regulates Cardiac Membrane Excitability and Physiology

Jerry Curran[1,3], **Michael A. Makara**[1,3], **Sean C. Little**[1,3], **Hassan Musa**[1,3], **Bin Liu**[1,3], **Xiangqiong Wu**[1], **Iuliia Polina**[1], **Joe Alecusan**[1], **Patrick Wright**[1,3], **Jingdong Li**[1], **George E. Billman**[1,3], **Penelope A. Boyden**[5], **Sandor Gyorke**[1,3], **Hamid Band**[6], **Thomas J. Hund**[1,4], and **Peter J. Mohler**[1,2,3]

[1]The Ohio State University Wexner Medical Center, The Dorothy M. Davis Heart & Lung Research Institute

[2]Department of Internal Medicine, Columbus, OH

[3]Department of Physiology and Cell Biology, Columbus, OH

[4]The Ohio State University College of Engineering, Department of Biomedical Engineering, Columbus, OH

[5]Department of Pharmacology and Center for Molecular Therapeutics, Columbia University Medical Center, New York, NY

[6]The Eppley Institute and UNMC-Eppley Cancer Center, University of Nebraska Medical Center, Omaha, NE

Abstract

Rationale—Cardiac function is dependent on the coordinate activities of membrane ion channels, transporters, pumps, and hormone receptors to dynamically tune the membrane electrochemical gradient in response to acute and chronic stress. While our knowledge of membrane proteins has rapidly advanced over the past decade, our understanding of the subcellular pathways governing the trafficking and localization of integral membrane proteins is limited, and essentially unstudied in vivo. In heart, to our knowledge, there are no in vivo mechanistic studies that directly link endosome-based machinery with cardiac physiology.

Objective—Define the in vivo roles of endosome-based cellular machinery for cardiac membrane protein trafficking, myocyte excitability, and cardiac physiology.

Methods and Results—We identify the endosome-based EHD3 pathway as essential for cardiac physiology. EHD3$^{-/-}$ hearts display structural and functional defects including bradycardia and rate variability, conduction block, and blunted response to adrenergic stimulation. Mechanistically, EHD3 is critical for membrane protein trafficking, as EHD3$^{-/-}$ myocytes display

Address correspondence to: Dr. Peter Mohler, The Ohio State University Wexner Medical Center, The Dorothy M. Davis Heart & Lung Research Institute, 473 W. 12th Ave., Columbus, OH 43230, Phone: 614-292-5019, Fax: 614-247-7799, peter.mohler@osumc.edu; Dr. Jerry Curran, The Ohio State University Wexner Medical Center, The Dorothy M. Davis Heart & Lung Research Institute, 473 W. 12th Ave., Columbus, OH 43230, Phone: 614-292-5019, Fax: 614-247-7799, jerry.curran@osumc.edu.

DISCLOSURES
None

reduced expression/localization of Na/Ca exchanger and $Ca_v1.2$ with a parallel reduction in I_{NCX} and $I_{Ca,L}$. Functionally, EHD3$^{-/-}$ myocytes show increased sarcoplasmic reticulum [Ca], increased spark frequency, and reduced expression/localization of ankyrin-B, a binding partner for EHD3 and Na/Ca exchanger. Finally, we show that in vivo EHD3$^{-/-}$ defects are due to cardiac-specific roles of EHD3 as mice with cardiac-selective EHD3 deficiency demonstrate both structural and electrical phenotypes.

Conclusions—These data provide new insight into the critical role of endosome-based pathways in membrane protein targeting and cardiac physiology. EHD3 is a critical component of protein trafficking in heart and is essential for the proper membrane targeting of select cellular proteins that maintain excitability.

Keywords

EHD3; protein trafficking; cell biology; ankyrin; cell physiology; ion channel; electrophysiology; mice

INTRODUCTION

Highly evolved and differentiated for excitation-contraction (EC) coupling, cardiac myocytes express a specific profile of ion channels, pumps, and transporters that maintain cardiomyocyte electrical excitability. Collectively, these membrane proteins mediate action potential (AP) formation and response, Ca-induced Ca release (CICR), and the secretion of natriuretic peptides.[1, 2] Equally important is the set of hormone receptors localized to the sarcolemmal (SL) membrane that regulate the activity and response of ion channels and pumps through specific second messenger pathways. These highly evolved systems are tightly synchronized to tune cardiac output to meet the changing demands placed on the heart by variable stresses. Like other complex cells, cardiac membrane protein residency is in constant flux, and primarily regulated by three general processes including synthesis and trafficking of new proteins through the endoplasmic reticulum and Golgi to specific membrane domains, membrane protein internalization and recycling, and ultimate membrane protein degradation. In metazoan cells, endosome-based protein machinery is indispensable for each of these functions. However, we know little to nothing about the in vivo components of the cardiac endosome system. The Eps15 homology domain (EHD)-containing protein family (EHD1-4) mediates endosome-based trafficking in non-excitable and heterologous cells.[3-5] Recently, we identified EHD3 in human heart.[6] Further, we identified that EHD3 levels are elevated in multiple forms of cardiovascular disease.[7] Based on our initial findings, we hypothesized that the endosome-based EHD3 protein plays critical roles in cardiac membrane protein trafficking and physiology at baseline and in disease, and that EHD3 deficiency would result in defects in both cardiac electrical and functional phenotypes.

Here, we define the in vivo physiological and mechanistic roles of EHD3 in the heart. EHD3-deficient (EHD3$^{-/-}$) mice display enlarged hearts and abnormal cardiac function. Furthermore, EHD3$^{-/-}$ mice exhibit bradycardia, atrioventricular (AV) conduction block, heart rate (HR) variability, and have a blunted response to beta-adrenergic receptor (β-AR) stimulation. Adult ventricular myocytes isolated from EHD3$^{-/-}$ mouse hearts display a

significant attenuation of action potential duration (APD), increased sarcoplasmic reticulum Ca ($[Ca]_{SRT}$) and Ca sparks, a blunted β-AR response, and reduced expression and function of the L-type Ca channel ($Ca_v1.2$) and Na/Ca exchanger (NCX). Confocal studies revealed improper localization of both the $Ca_v1.2$ and NCX, consistent with the role of EHD3 for targeting select membrane proteins. Moreover, ankyrin-B, an intermediate binding partner between EHD3 and the NCX, is decreased in EHD3$^{-/-}$ mice providing the underlying mechanism between EHD3 and membrane proteins. Finally, EHD3$^{-/-}$ defects are due to cardiac-intrinsic roles of EHD3 as mice with cardiac-specific EHD3 deficiency demonstrate structural and electrical phenotypes. These new data define a critical role for EHD3 in select protein trafficking in heart as well as indicate the importance for subcellular protein targeting for cardiac excitability.

METHODS

For complete, expanded methods please refer to the Online Supplement. All animal studies were performed in accordance with the American Physiological Society Guiding Principles for Research Involving Animals and Human Beings, and approved by The Ohio State University Institutional Animal Care and Use Committee. The investigation conforms to the *Guide for the Care and Use of Laboratory Animals* published by the US National Institutes of Health (NIH Publication No. 85-23, revised 1996).

Echocardiography

Transthoracic echocardiogram was performed on anesthetized WT and EHD3$^{-/-}$ mice as previously described[7] to measure the in vivo function of the heart.

Electrophysiology

Whole-cell recordings were obtained at RT with the use of standard patch-clamp techniques, and cells from the WT and EHD3$^{-/-}$ groups had a similar membrane capacitance (Online Figure I).[8]

ECG experiments

ECG recordings of ambulatory mice were obtained using subcutaneously implanted radiotelemeters (DSI, St. Paul, MN).[9] Recordings were obtained from mice that were conscious, post-exercise, post-isoprenaline injection, and post-exercise plus isoprenaline injection. For baseline HR analysis, continuous ECG data was collected from WT and EHD3$^{-/-}$ mice for 1 hour. Recordings were performed every 48 hours at the same time of day. For stress tests, mice were run on a treadmill for a maximum of 45 minutes or until exhaustion, then immediately injected with isoprenaline (0.5 mg/kg). Non-sustained and sustained arrhythmias were identified using standard ECG analysis guidelines.[10]

In a separate group of mice than those implanted with radiotelemeters, surface ECG recordings were obtained under anesthesia with 1-2% isoflurane. Three needle electrodes were placed subcutaneously in the standard limb configuration. For each mouse, 15 min of continuous data were sampled at 4 kHz with a PowerLab 4/30 interface (AD Instruments,

Colorado Springs, CO). Analysis was performed offline using LabChart 7 Pro (AD Instruments).

SR Ca load

SR Ca load and Ca handling were assessed from isolated ventricular myocytes as previously described.[11] $[Ca]_{SRT}$ was calculated through the pseudo-ratio as previously described[11] with $[Ca]_d$ assumed to be 120 nM for all mice.

Generation of EHD3$^{-/-}$ mouse

EHD3$^{-/-}$ mice were generated as previously described.[12] DNA was isolated from tail clips of 10 day old mice, and mice were genotyped by PCR. Three primers in a single duplex PCR reaction amplified the WT allele (377 bp) and the deleted allele (488 bp, Figure 1A). To test the in vivo cardiac-intrinsic roles of EHD3, we utilized a conditional null mutant allele where the 5′ UTR and exon 1 of the mouse EHD3 gene (*Ehd3*) were flanked by LoxP sites (*Ehd3*$^{f/f}$) and therefore are deleted in the presence of Cre recombinase. We selectively eliminated EHD3 in cardiomyocytes by utilizing αMHC-Cre knock-in mice[13]; homozygous conditional knockout mice are referred to as αMHC-Cre; *Ehd3*$^{f/f}$ or cKO. Mice displayed lack of EHD3 by PCR and immunoblot. Mice were born at expected Mendelian ratios, were healthy and fertile with body weights comparable to their wild-type littermates.

Antibodies

The following antibodies were used to conduct this study: affinity-purified rabbit polyclonal antibody directed at human EHD4 (SHRKSLPKAD), rabbit polyclonal anti-EHD1 (abcam, Cambridge, MA), mouse monoclonal anti-NCX1 (Swant, Bellinzona, Switzerland), rabbit polyclonal anti-ankyrin-B[14], mouse monoclonal anti-$Ca_v1.2$[15], rabbit polyclonal anti-β_1- and anti-β_2-adrenergic receptor (Santa Cruz Biotechnology, Dallas, TX), rabbit polyclonal anti-$Na_v1.5$[16], actin (Santa Cruz Biotechnology), rabbit polyclonal anti-SERCA (Santa Cruz), mouse monoclonal anti-phospholamban (abcam, Cambridge, MA), rabbit monoclonal anti-calsequestrin2 (abcam).

Immunoblots and immunostaining

Immunoblots of whole heart lysates were performed as described.[17] Briefly, whole hearts were harvested from WT and EHD3$^{-/-}$ adult, age-matched littermates and immediately placed into ice cold homogenization buffer (in mM: 50 Tris-HCl, 10 NaCl, 320 sucrose, 5 EDTA, 2.5 EGTA; supplemented with 1:1000 protease inhibitor cocktail and 1:1000 PMSF [Sigma]). Following quantification, tissue lysates were analyzed on Mini-PROTEAN tetra cell (BioRad) on a 4-15% precast TGX gel (BioRad). Gels were transferred to a nitrocellulose membrane using the Mini-PROTEAN tetra cell (BioRad). Membranes were blocked for 1 hour at room temperature using a 3% BSA solution or 5% milk solution and incubated with primary antibody overnight at 4°C. Densitometry analysis was done using ImageLab software (BioRad). For all experiments, protein values were normalized against an internal loading control (actin or GAPDH).

Statistics

All values are presented as mean ± SEM. When appropriate, data were analyzed using a two-tailed Students t-test. I_{NCX} values were analyzed using a one-tail Student t-test with the WT myocytes predicted to have the larger mean value based on previous work. [6] P-values <0.05 were considered significant.

RESULTS

EHD3$^{-/-}$ mice display chamber dilation and reduced ejection fraction

To evaluate the role of EHD3 in cardiac physiology, we first examined the structure and function of the heart in EHD3$^{-/-}$ and WT mice (Figure 1A). By gross examination, whole heart morphology was significantly altered in EHD3$^{-/-}$ mice. Both atria and ventricles were larger in excised EHD3$^{-/-}$ hearts compared to those of WT littermates (Figure 1B) and we observed increased heart weight to body weight ratio in EHD3$^{-/-}$ mice compared to WT littermates (EHD3$^{-/-}$: 7.98 mg/g ± 0.26; WT: 6.79 mg/g ± 0.21, p=0.004, Online Table I). We performed echocardiograms on age-matched WT and EHD3$^{-/-}$ mice to directly assess if EHD3-deficiency affected the development, structure, or contractility of the adult heart. Both fractional shortening (FS) and ejection fraction (EF) were decreased in EHD3$^{-/-}$ mice (Figure 1F-G), though stroke volume (SV) was preserved (Figure 1H; likely due to a larger left ventricular (LV) diameter in EHD3$^{-/-}$ hearts [Figure 1C]). Both anterior and posterior systolic wall thicknesses were decreased in EHD3$^{-/-}$ mice (Figure 1D-E), however we observed no difference in diastolic wall thickness between genotypes. Chamber dilation and SV phenotypes were present in EHD3$^{-/-}$ mice as early as four weeks, although at this age we observed no difference in FS or EF between genotypes (Online Table I-II).

EHD3$^{-/-}$ mice display bradycardia, heart rate variability, and cardiac conduction defects

We next assessed the in vivo role of EHD3 in cardiac electrical signaling. ECG data were acquired from conscious, ambulatory WT and EHD3$^{-/-}$ mice with subcutaneously implanted radiotelemeters. Notably, we observed a significant reduction in baseline heart rate in EHD3$^{-/-}$ mice and WT littermates (Figure 2A). We examined HR variability by conducting a fast Fourier transform analysis of HR. In addition to bradycardia, EHD3$^{-/-}$ mice displayed increased HR variability compared with controls, with the frequency of lower heart rates more prominent in EHD3$^{-/-}$ mice (Figure 2B-C). Analysis of individual ECG traces revealed numerous electrical phenotypes in EHD3$^{-/-}$ mice. Unlike WT mice (Figure 2D-E), EHD3$^{-/-}$ mice were prone to bursts of irregular heart rate reflected as increased variability in the R to R interval (RR_i) and sinus pause in selected segments of the ECG recordings (Figure 2C). EHD3$^{-/-}$, but not WT mice commonly displayed significant RR_i variability for periods lasting more than 1 minute and as long as 5 minutes under baseline conditions. This phenotype became even more apparent when EHD3$^{-/-}$ mice were stimulated with isoprenaline (Iso) injection (Figure 2E). With the exception of episodes of sinus pause or AV block, we did not observe significant differences in either P-R interval or QRS duration between WT and EHD3$^{-/-}$ mice (Online Figure II).

In addition to increased RR variability, EHD3$^{-/-}$ mice consistently displayed type II AV conduction block, with exacerbation of the phenotype following Iso stimulation (Figure 2F).

The type II block was characterized by two P waves without subsequent QRS complexes followed by a single extended R-R interval and resumption of normal rhythm (Figure 2F). This pattern of AV block was maintained for as long as 15 minutes in EHD3$^{-/-}$ mice and was never observed in WT littermates. Collectively, we conclude that normal cardiac automaticity and conduction require EHD3.

EHD proteins have been implicated in membrane receptor expression, internalization, and recycling in other cell systems.[5, 18, 19] We therefore assessed the impact of EHD3 deficiency on β-adrenergic receptor (AR) signaling in vivo. In conscious mice the maximum HR in response to Iso injection (either low or high dose) was equivalent in WT and EHD3$^{-/-}$ mice; however, the duration of this response was significantly shorter in the EHD3$^{-/-}$ mice (Online Figure IIIA-B). To limit any variation in the data resulting from the physical handling of the mice, we performed surface ECG recordings on sedated mice with continuous monitoring of HR (Online Figure IIIC). After injection of Iso (0.5 mg/kg), WT mice had a significantly larger increase in HR compared to EHD3$^{-/-}$ mice (79 ± 10 vs. 46 ± 5 bpm; $p<0.05$; Online Figure IIID). Outside of the sinus pause and AV block we observed no other evidence of arrhythmias (i.e. premature ventricular complexes, or atrial flutter or fibrillation) in EHD3$^{-/-}$ mice at baseline, following Iso injection, or Iso injection and exercise.

Based on these data, we hypothesized that EHD3$^{-/-}$ myocytes would display altered β_1-AR trafficking and membrane expression. However, by immunoblot, we observed increased expression of β_1- and β_2-ARs in EHD3$^{-/-}$ hearts (Online Figure IIIE-H). As immunoblots are unable to discriminate between proteins embedded in the surface membrane and those confined to internal compartments (including endosomes), we utilized radiolabeled β_1-AR-specific antagonist, ^{3}H-CGP-12177, to assay potential changes in cell surface β_1-AR density in intact, isolated ventricular cardiomyocytes. Using this assay, we observed no significant difference in β_1-AR surface density (Online Figure III-I). Notably, however, by immunostaining and confocal analysis of WT and EHD3$^{-/-}$ adult ventricular cardiomyocytes, we observed a significant population of β_1-AR expression in the peri-nuclear region of EHD3-deficient myocytes (Online Figure IIIJ). Based on these data, we hypothesize that while anterograde membrane trafficking of the β_1-AR is EHD3-independent, β_1-AR endosomal recycling may be compromised in EHD3-deficient myocytes.

EHD3$^{-/-}$ myocytes display abnormal myocyte excitability

We directly evaluated the effect of EHD3 deficiency on cardiomyocyte membrane excitability. APD was significantly shorter in ventricular myocytes isolated from EHD3$^{-/-}$ hearts (Figure 3A-B,D; n=7, both WT and EHD3$^{-/-}$). At all intervals, APD was significantly shorter in EHD3$^{-/-}$ myocytes, though the shortening was most significant in the early phases of the AP (APD_{50} and APD_{75}, Figure 3A-B,D). Further, consistent with in vivo data, EHD3$^{-/-}$ myocytes displayed a blunted beta-adrenergic response to Iso treatment (100 nM) compared with WT littermates (Figure 3C-E).

EHD3$^{-/-}$ myocytes display increased SR Ca load and Ca spark frequency

Given the abbreviated action potential, but no reduction of the stroke volume in EHD3$^{-/-}$ mice, we hypothesized that EHD3$^{-/-}$ myocytes may have an increased SR Ca load ($[Ca]_{SRT}$). This higher Ca load would increase the Ca sensitivity of the SR Ca release channel, ryanodine receptor (RyR), making it more prone to release even with a smaller Ca trigger, similar to the physiological mechanism underlying increased contractility during catecholamine stimulation. [20] To test this hypothesis we field stimulated isolated cardiac myocytes at 0.5 Hz and assessed $[Ca]_{SRT}$ using caffeine-stimulated Ca release.[11] Figure 4 shows that no differences in $[Ca]_i$ transients were observed between WT and EHD3$^{-/-}$ myocytes (Figure 4A-D), even though there was a significant increase in $[Ca]_{SRT}$ in the latter (186 ± 25 vs. 262 ± 20 μM, Figure 4E). Increased Ca sensitivity of the RyR is further reflected by an increased spark frequency found in intact ventricular EHD3$^{-/-}$ myocytes (Figure 4F-H). These data support the hypothesis that $[Ca]_{SRT}$ is up-regulated in order to maintain contractility in EHD3$^{-/-}$ myocytes indicating a role for EHD3 in Ca homeostasis.

EHD3 is required for Na/Ca exchanger and $Ca_v1.2$ membrane targeting in heart

As a first step toward determining the ionic basis for reduced APD, increased SR Ca^{2+} load, and increased spark frequency in EHD3$^{-/-}$ myocytes, we screened for likely candidates by performing parameter sensitivity analysis on a well-validated mathematical model of the mouse ventricular AP (Online Figure IV). This analysis revealed that, among sarcolemmal ion channels/transporters, the L-type Ca^{2+} current and Na/Ca exchanger (NCX) had the greatest influence on APD and SR Ca^{2+} load, respectively, in a manner consistent with experimentally measured changes. More specifically, the model predicts that loss of L-type Ca^{2+} channel membrane targeting would produce the greatest decrease in APD while loss of NCX would result in the greatest increase in SR Ca^{2+} load.

Based on WT and EHD3$^{-/-}$ APD and $[Ca]_{SRT}$ data, and subsequent mathematical predictions, we first evaluated the expression of NCX and $Ca_v1.2$ by immunoblot. $Ca_v1.2$ and NCX expression were reduced by 24% and 17%, respectively (Figure 5A-B, $p<0.05$). Conversely, no differences in SERCA2, phospholamban, or calsequestrin expression were identified between genotypes (Online Figure V). Together with computational analysis, these results provide a possible mechanism for abnormal AP and SR Ca^{2+} properties in EHD3$^{-/-}$ myocytes.

Decreased expression of NCX and $Ca_v1.2$ was paralleled by decreased membrane expression of both NCX and $Ca_v1.2$ in EHD3$^{-/-}$ mice by immunostaining and confocal analysis of isolated ventricular cardiomyocytes. Representative images are shown in Figures 5C-H. In WT myocytes, the NCX clearly localizes to both the SL membrane and along the transverse-tubule network (Figure 5C,E). However, in EHD3$^{-/-}$ myocytes, the localization to these two domains is decreased with a striking peri-nuclear distribution that is not observed in WT cells (Figure 5D,F).

$Ca_v1.2$ localization was also disrupted by EHD3 deficiency. In WT myocytes, $Ca_v1.2$ staining shows a typical striated pattern (Figure 5G).[21] This pattern was disrupted in EHD3$^{-/-}$ myocytes (Figure 5H). While some striations were evident, $Ca_v1.2$-dependent

staining was largely diffuse and not localized to any specific subcellular domain. Using an antibody specific for N-cadherin and the lipophilic membrane marker, di-8-ANEPPS, we observed no structural changes to intercalated disc and the t-tubule system in EHD3$^{-/-}$ myocytes, indicating that myocyte ultrastructure is EHD3-independent (Figure 5I-L).

Finally, to quantitate potential functional differences, Na/Ca exchanger (I_{NCX}) and $Ca_v1.2$ ($I_{Ca,L}$) currents were assessed in isolated ventricular myocytes using whole-cell patch clamp. Data in Figure 5M-Q show that both $I_{Ca,L}$ and I_{NCX} were significantly reduced in EHD3$^{-/-}$ myocytes. I_{NCX} was significantly decreased in EHD3-deficient myocytes compared to that in WT myocytes with a 47% reduction in peak current (Figure 5M-N). At baseline, $I_{Ca,L}$ was decreased 60% in EHD3$^{-/-}$ myocytes (Figure 5O,Q). Treatment with Iso (100 nM) increased $I_{Ca,L}$ similarly in both WT and EHD3$^{-/-}$ myocytes (Figure 5P-Q).

In summary, our data obtained using three different approaches support a mechanistic in vivo role of EHD3 for the membrane targeting of both Na/Ca exchanger and the $Ca_v1.2$ in primary adult cardiomyocytes. Importantly, loss of membrane protein expression phenotypes were EHD3-dependent (versus a compensatory response to a failing myocardium) as we observed defects in channel or transporter expression in EHD3$^{-/-}$ primary cardiomyocytes (Online Figure VI) isolated at post-natal day 1 (weeks prior to observed functional phenotypes).

Dysregulated ankyrin-B trafficking in EHD3$^{-/-}$ myocytes

Our findings implicate EHD3 for targeting select ion channels/transporters to the myocyte membrane. However, to further understand the mechanistic link between EHD3 and membrane protein targeting, we investigated the regulation of ankyrin-B, a membrane adapter protein previously linked with both NCX and EHD3. [6, 22-24] Notably, ankyrin-B expression is significantly decreased (~40%) in EHD3$^{-/-}$ hearts (Figure 6A-B). Furthermore, EHD3$^{-/-}$ myocytes show altered ankyrin-B staining. We observed a decrease in overall intensity with increased peri-nuclear ankyrin-B staining in EHD3$^{-/-}$ myocytes compared to WT myocytes (Figure 6C-J). Defects in ankyrin-B expression and localization are present from birth and are directly EHD3-dependent, as viral re-introduction of GFP-EHD3 is sufficient to rescue the expression of ankyrin-B in EHD3$^{-/-}$ myocytes (Online Figure VII). Based on these findings, we predict that that ankyrin-B plays a key nodal role for EHD3-dependent membrane targeting in heart.

Cardiac-specific EHD3$^{-/-}$ mice display structural and electrical phenotypes

Global EHD3$^{-/-}$ mice display bradycardia, HR variability, conduction defects, and structural phenotypes (Figures 1-2). However, these parameters may be influenced by cardiac extrinsic factors (i.e. nervous system). To directly test the in vivo cardiac-intrinsic roles of EHD3, we utilized a conditional null mutant allele where exon 1 of the mouse EHD3 gene (*Ehd3*) was flanked by LoxP sites (*Ehd3$^{f/f}$*) and therefore are deleted in the presence of Cre recombinase. We selectively eliminated EHD3 in cardiomyocytes by utilizing αMHC-Cre knock-in mice[13]; homozygous conditional knockout mice are referred to as αMHC-Cre; *Ehd3$^{f/f}$* or cKO.

Data presented in Figure 7 demonstrate a striking similarity between the EHD3$^{-/-}$ and the EHD3$^{-/-}$ cKO mice. Resting HR was equally depressed in the EHD3$^{-/-}$ cKO and EHD3$^{-/-}$ mice compared to WT (Figure 7A, $p<0.05$) with a shifted distribution of HR similar to the EHD3$^{-/-}$ model (Figure 7B). Moreover, we observed similar conduction defects in the EHD3$^{-/-}$ cKO mice: a high HR variability at baseline (Figure 7C)**,** a high incidence of SAN pause (Figure 7D), and AV conduction block (Figure 7E) following Iso treatment. SAN pause and AV block were also present at a lower rate in the absence of Iso stimulation (not shown). These conduction disorders were never observed in the WT mice. Importantly, at the level of the single myocyte, cKO mouse myocytes display significant loss of I_{NCX} and $I_{Ca,L}$ (Figure 7F-I). Specifically, EHD3$^{-/-}$ cKO peak I_{NCX} was reduced ~43%, and $I_{Ca,L}$ was reduced ~53% compared to WT (both $p<0.001$). Beyond electrical phenotypes, the structural and function phenotype of EHD3$^{-/-}$ global and cKO mice assessed by echocardiography were similar in nearly all respects (Online Table III). Together, these new data indicate that cardiac EHD3 is critical for normal cardiac structural and electrical phenotypes. Further, these data support cardiac intrinsic roles for EHD3 in regulating normal cardiac structure and function.

DISCUSSION

Anterograde and retrograde protein trafficking and endocytic protein recycling are often overlooked cellular systems. As an often membrane-centric discipline, we take for granted that these pathways are present and critical for cell function. Our lack of understanding may stem from the particular difficulties in studying these systems, as endosomes undergo an incredibly complex maturation process that makes investigating particular processes or steps within these pathways problematic, particularly in vivo. Relatively little is known about the particular proteins and enzymes that may be involved in cell membrane trafficking processes. Research over the last 15 years has only just started to isolate single proteins and enzymes that are involved in trafficking. Proteins like Arf6, SNARE complexes, BIN1, EHD1-4, amongst others are now the focus of efforts to further understand protein trafficking in all cell types.[4, 25-27] Recently, a mutation in EHD3 was linked to major depressive disorder in humans, indicating that trafficking systems simply do not maintain cellular health but may be the primary cause for medical disorders.[28] We recently identified EHD3 in the heart and demonstrated an association of this protein with cardiac disease.[7]

This report is the first to detail the functional in vivo roles of EHD3 in the heart. The key findings of this investigation are: 1) EHD3$^{-/-}$ hearts are significantly larger with preserved cardiac output; 2) EHD3$^{-/-}$ mice display bradycardia, heart rate variability, type II conduction block, and a blunted response to β-AR stimulation; 3) isolated EHD3$^{-/-}$ myocytes display a significantly abbreviated APD and a blunted response to β-AR stimulation; 4) EHD3$^{-/-}$ myocytes have a significant reduction in expression, targeting, and function of $Ca_v1.2$ and NCX; 5) EHD3$^{-/-}$ myocytes display a significantly larger $[Ca]_{SRT}$ and a higher frequency of sparks compared to WT; 6) ankyrin-B function is directly altered by EHD3 loss; and 7) EHD3$^{-/-}$ phenotypes can be directly linked with EHD3 expressed in myocytes. Together, these data highlight the importance of endosome-based pathways for normal cardiac function.

EHD proteins (EHD1-4) are key regulators of membrane protein targeting in other tissue and cell types.[29-31] This family of proteins has high homology amongst the members (ranging from 71-86%), with EHD1 and EHD3 sharing the highest homology.[32] This degree of homology infers similar and potentially redundant cellular function. For example, in a *C. elegans* model lacking the EHD ortholog, RME-1, expression of human EHD1-4 is sufficient to rescue RME-1-dependent protein trafficking.[4] These findings appear relevant to our study. For example, while select protein trafficking pathways are disrupted and EHD3$^{-/-}$ hearts display multiple in vivo phenotypes, the viability of EHD3$^{-/-}$ mice strongly support that additional pathways are present for ion channel and transporter membrane expression. Interestingly, EHD1 expression was significantly up-regulated in the EHD3$^{-/-}$ mice (Online Figure VIII). We speculate that this up-regulation may represent a compensatory response of the heart to maintain protein trafficking. We also observed reduced expression of EHD4 in the EHD3$^{-/-}$ hearts (Online Figure VIII). While nothing is currently known regarding the role of either EHD1 or EHD4 proteins in heart, these data suggest that the EHD family may collaborate to regulate endosome-based trafficking pathways.

EHD3$^{-/-}$ and EHD3$^{-/-}$ cKO mice display bradycardia, rate variability, and conduction defects. The sinoatrial node (SAN) is the pacemaker of the heart, and the atrioventricular node (AVN) is critical for the proper conduction of the AP from the atria to the ventricles. Both the SAN and AVN depend on voltage-gated ion channels and exchangers to maintain proper electrical activity. In particular, the SAN is known to rely on both the $I_{Ca,L}$ and I_{NCX} for automaticity; while $I_{Ca,L}$ activity in the AVN is thought to be indispensable for conduction through this junction.[33-36] Notably, EHD3 is expressed in the SAN of both mice and canine hearts (Online Figure IX). While additional studies will be necessary to identify specific roles of EHD3 in these critical cardiac cell types, our initial findings link EHD3 function with cardiac automaticity.

EHD3-dependent trafficking in the heart may represent a nodal control pathway for regulating protein trafficking in response to acute or chronic stress. Here we demonstrate that EHD3-dependent mechanisms are broadly implicated in the subcellular trafficking and localization of many of the proteins involved in EC coupling. Na/Ca exchanger expression is increased in nearly all reports examining protein expression in HF, including in humans.[37, 38] While initially compensatory, as the severity of HF progresses the increased Na/Ca exchanger expression becomes maladaptive and arrhythmogenic leading to delayed after-depolarizations.[39, 40] We previously reported that EHD3 expression is increased in numerous etiologies of HF.[7] The evidence in this report strongly indicates that EHD3 mediates NCX trafficking in the heart. Together, I_{NCX} and $I_{Ca,L}$ make up a substantial fraction of the whole cell current during a typical action potential. Based on modeling predictions, we expect that loss of I_{CaL} plays a critical role in abbreviation of APD in EHD3-null myocytes, especially in the early phases of AP development, while loss of I_{NCX} determines changes in SR Ca^{2+} load. While EHD3 is critical for NCX, $Ca_v1.2$, and ankyrin-B targeting, it is important to note that EHD3 also likely targets additional membrane proteins, and that observed phenotypes in the EHD3$^{-/-}$ heart may not be related to calcium-based signaling pathways. Future experiments will be critical to define the full spectrum of EHD3 targets in heart.

Finally, additional work will be necessary to define the structural phenotypes observed in EHD3$^{-/-}$ hearts during development, as well as the relationship between structural and electrical phenotypes. Despite chamber dilation, reduced EF, and reduced SV, the myopathy phenotype in EHD3$^{-/-}$ mice is complex and may not simply represent a pure maladaptive or physiological hypertrophy phenotype. In fact, despite observing increased expression of slow skeletal muscle troponin (consistent with maladaptive hypertrophy, $p<0.05$), we did not observe elevated expression of ANP, BNP, or β-myosin heavy chain expression mRNA in EHD3$^{-/-}$ hearts (p=N.S.). Future experiments will be critical to fully characterize the role of EHD3 in cardiac development as well as the specific roles of EHD3 in heart failure. Importantly, EHD3$^{-/-}$ NCX targeting phenotypes were directly due to EHD3 deficiency, and not a compensatory response to functional decompensation, as dysregulated NCX targeting was present from birth, and rhythm defects were observed as early as 4 weeks of age in EHD3$^{-/-}$ mice (prior to depressed cardiac function; Online Figures VI & X). Thus, our data support that that EHD3 plays roles in targeting proteins involved in both cardiac structural and electrical functions.

Supplementary Material

Refer to Web version on PubMed Central for supplementary material.

Acknowledgments

SOURCES OF FUNDING

This work was supported by the National Institutes of Health [HL114252 to JC]; [HL084583, HL083422, HL114383 to PJM]; [CA105489, CA87986, CA99163, and CA116552 to HB]; [HL096805, HL114893 to TJH]; Saving Tiny Hearts Society (PJM), and American Heart Association (PJM).

Nonstandard Abbreviations and Acronyms

AP	action potential
APD	action potential duration
β-AR	beta-adrenergic receptor
bpm	beats per minute
$[Ca]_i$	cytosolic Ca concentration
$[Ca]_{SRT}$	total sarcoplasmic reticulum Ca concentration
CaV1.2	L-type Ca channel type 1.2
CICR	Ca-induced Ca release
EC coupling	excitation-contraction coupling
EHD	Eps15 homology domain
ERC	endosomal recycling compartment
HF	heart failure
HR	heart rate

$I_{Ca,L}$	L-type Ca channel mediated membrane current
I_{NCX}	Na/Ca exchanger-mediated membrane current
Iso	isoprenaline
NCX	Na/Ca exchanger
RR_i	R to R interval
SL	sarcolemmal

REFERENCES

1. Bers DM. Cardiac excitation-contraction coupling. Nature. 2002; 415:198–205. [PubMed: 11805843]
2. Thibault G, Amiri F, Garcia R. Regulation of natriuretic peptide secretion by the heart. Annu Rev Physiol. 1999; 61:193–217. [PubMed: 10099687]
3. Caplan S, Naslavsky N, Hartnell LM, Lodge R, Polishchuk RS, Donaldson JG, Bonifacino JS. A tubular ehd1-containing compartment involved in the recycling of major histocompatibility complex class i molecules to the plasma membrane. Embo J. 2002; 21:2557–2567. [PubMed: 12032069]
4. George M, Ying G, Rainey MA, Solomon A, Parikh PT, Gao Q, Band V, Band H. Shared as well as distinct roles of ehd proteins revealed by biochemical and functional comparisons in mammalian cells and c. Elegans. BMC cell biology. 2007; 8:3. [PubMed: 17233914]
5. Naslavsky N, Rahajeng J, Sharma M, Jovic M, Caplan S. Interactions between ehd proteins and rab11-fip2: A role for ehd3 in early endosomal transport. Mol Biol Cell. 2006; 17:163–177. [PubMed: 16251358]
6. Gudmundsson H, Hund TJ, Wright PJ, Kline CF, Snyder JS, Qian L, Koval OM, Cunha SR, George M, Rainey MA, Kashef FE, Dun W, Boyden PA, Anderson ME, Band H, Mohler PJ. Eh domain proteins regulate cardiac membrane protein targeting. Circ Res. 2010; 107:84–95. [PubMed: 20489164]
7. Gudmundsson H, Curran J, Kashef F, Snyder JS, Smith SA, Vargas-Pinto P, Bonilla IM, Weiss RM, Anderson ME, Binkley P, Felder RB, Carnes CA, Band H, Hund TJ, Mohler PJ. Differential regulation of ehd3 in human and mammalian heart failure. J Mol Cell Cardiol. 2012; 52:1183–1190. [PubMed: 22406195]
8. Le Scouarnec S, Bhasin N, Vieyres C, Hund TJ, Cunha SR, Koval O, Marionneau C, Chen B, Wu Y, Demolombe S, Song LS, Le Marec H, Probst V, Schott JJ, Anderson ME, Mohler PJ. Dysfunction in ankyrin-b-dependent ion channel and transporter targeting causes human sinus node disease. Proc Natl Acad Sci U S A. 2008; 105:15617–15622. [PubMed: 18832177]
9. DeGrande S, Nixon D, Koval O, Curran JW, Wright P, Wang Q, Kashef F, Chiang D, Li N, Wehrens XH, Anderson ME, Hund TJ, Mohler PJ. Camkii inhibition rescues proarrhythmic phenotypes in the model of human ankyrin-b syndrome. Heart Rhythm. 2012; 9:2034–2041. [PubMed: 23059182]
10. Mitchell GF, Jeron A, Koren G. Measurement of heart rate and q-t interval in the conscious mouse. Am J Physiol. 1998; 274:H747–751. [PubMed: 9530184]
11. Curran J, Hinton MJ, Rios E, Bers DM, Shannon TR. Beta-adrenergic enhancement of sarcoplasmic reticulum calcium leak in cardiac myocytes is mediated by calcium/calmodulin-dependent protein kinase. Circulation research. 2007; 100:391–398. [PubMed: 17234966]
12. George M, Rainey MA, Naramura M, Foster KW, Holzapfel MS, Willoughby LL, Ying G, Goswami RM, Gurumurthy CB, Band V, Satchell SC, Band H. Renal thrombotic microangiopathy in mice with combined deletion of endocytic recycling regulators ehd3 and ehd4. PLoS ONE. 2011; 6:e17838. [PubMed: 21408024]
13. Agah R, Frenkel PA, French BA, Michael LH, Overbeek PA, Schneider MD. Gene recombination in postmitotic cells. Targeted expression of cre recombinase provokes cardiac-restricted, site-

specific rearrangement in adult ventricular muscle in vivo. J Clin Invest. 1997; 100:169–179. [PubMed: 9202069]

14. Abdi KM, Mohler PJ, Davis JQ, Bennett V. Isoform specificity of ankyrin-b: A site in the divergent c-terminal domain is required for intramolecular association. J Biol Chem. 2006; 281:5741–5749. [PubMed: 16368689]
15. Balijepalli RC, Foell JD, Hall DD, Hell JW, Kamp TJ. Localization of cardiac l-type ca(2+) channels to a caveolar macromolecular signaling complex is required for beta(2)-adrenergic regulation. Proc Natl Acad Sci U S A. 2006; 103:7500–7505. [PubMed: 16648270]
16. Hund TJ, Koval OM, Li J, Wright PJ, Qian L, Snyder JS, Gudmundsson H, Kline CF, Davidson NP, Cardona N, Rasband MN, Anderson ME, Mohler PJ. A beta(iv)-spectrin/camkii signaling complex is essential for membrane excitability in mice. J Clin Invest. 2010; 120:3508–3519. [PubMed: 20877009]
17. Kline CF, Wright PJ, Koval OM, Zmuda EJ, Johnson BL, Anderson ME, Hai T, Hund TJ, Mohler PJ. Betaiv-spectrin and camkii facilitate kir6.2 regulation in pancreatic beta cells. Proc Natl Acad Sci U S A. 2013; 110:17576–17581. [PubMed: 24101510]
18. Posey AD Jr. Swanson KE, Alvarez MG, Krishnan S, Earley JU, Band H, Pytel P, McNally EM, Demonbreun AR. Ehd1 mediates vesicle trafficking required for normal muscle growth and transverse tubule development. Dev Biol. 2014; 387:179–190. [PubMed: 24440153]
19. Guilherme A, Soriano NA, Furcinitti PS, Czech MP. Role of ehd1 and ehbp1 in perinuclear sorting and insulin-regulated glut4 recycling in 3t3-l1 adipocytes. J Biol Chem. 2004; 279:40062–40075. [PubMed: 15247266]
20. Gyorke I, Hester N, Jones LR, Gyorke S. The role of calsequestrin, triadin, and junctin in conferring cardiac ryanodine receptor responsiveness to luminal calcium. Biophys J. 2004; 86:2121–2128. [PubMed: 15041652]
21. Scriven DR, Dan P, Moore ED. Distribution of proteins implicated in excitation-contraction coupling in rat ventricular myocytes. Biophys J. 2000; 79:2682–2691. [PubMed: 11053140]
22. Li ZP, Burke EP, Frank JS, Bennett V, Philipson KD. The cardiac na+-ca2+ exchanger binds to the cytoskeletal protein ankyrin. J Biol Chem. 1993; 268:11489–11491. [PubMed: 8505285]
23. Cunha SR, Bhasin N, Mohler PJ. Targeting and stability of na/ca exchanger 1 in cardiomyocytes requires direct interaction with the membrane adaptor ankyrin-b. J Biol Chem. 2007; 282:4875–4883. [PubMed: 17178715]
24. Cunha SR, Mohler PJ. Cardiac ankyrins: Essential components for development and maintenance of excitable membrane domains in heart. Cardiovasc Res. 2006; 71:22–29. [PubMed: 16650839]
25. D'Souza-Schorey C, Li G, Colombo MI, Stahl PD. A regulatory role for arf6 in receptor-mediated endocytosis. Science. 1995; 267:1175–1178. [PubMed: 7855600]
26. Weber T, Zemelman BV, McNew JA, Westermann B, Gmachl M, Parlati F, Sollner TH, Rothman JE. Snarepins: Minimal machinery for membrane fusion. Cell. 1998; 92:759–772. [PubMed: 9529252]
27. Hong TT, Smyth JW, Gao D, Chu KY, Vogan JM, Fong TS, Jensen BC, Colecraft HM, Shaw RM. Bin1 localizes the l-type calcium channel to cardiac t-tubules. PLoS Biol. 2010; 8:e1000312. [PubMed: 20169111]
28. Shi C, Zhang K, Wang X, Shen Y, Xu Q. A study of the combined effects of the ehd3 and frem3 genes in patients with major depressive disorder. Am J Med Genet B Neuropsychiatr Genet. 2012; 159B:336–342. [PubMed: 22337703]
29. Daumke O, Lundmark R, Vallis Y, Martens S, Butler PJ, McMahon HT. Architectural and mechanistic insights into an ehd atpase involved in membrane remodelling. Nature. 2007; 449:923–927. [PubMed: 17914359]
30. Galperin E, Benjamin S, Rapaport D, Rotem-Yehudar R, Tolchinsky S, Horowitz M. Ehd3: A protein that resides in recycling tubular and vesicular membrane structures and interacts with ehd1. Traffic. 2002; 3:575–589. [PubMed: 12121420]
31. Miliaras NB, Wendland B. Eh proteins: Multivalent regulators of endocytosis (and other pathways). Cell biochemistry and biophysics. 2004; 41:295–318. [PubMed: 15475615]

32. Pohl U, Smith JS, Tachibana I, Ueki K, Lee HK, Ramaswamy S, Wu Q, Mohrenweiser HW, Jenkins RB, Louis DN. Ehd2, ehd3, and ehd4 encode novel members of a highly conserved family of eh domain-containing proteins. Genomics. 2000; 63:255–262. [PubMed: 10673336]
33. Mangoni ME, Couette B, Bourinet E, Platzer J, Reimer D, Striessnig J, Nargeot J. Functional role of l-type cav1.3 ca2+ channels in cardiac pacemaker activity. Proc Natl Acad Sci U S A. 2003; 100:5543–5548. [PubMed: 12700358]
34. Lyashkov AE, Juhaszova M, Dobrzynski H, Vinogradova TM, Maltsev VA, Juhasz O, Spurgeon HA, Sollott SJ, Lakatta EG. Calcium cycling protein density and functional importance to automaticity of isolated sinoatrial nodal cells are independent of cell size. Circ Res. 2007; 100:1723–1731. [PubMed: 17525366]
35. Marger L, Mesirca P, Alig J, Torrente A, Dubel S, Engeland B, Kanani S, Fontanaud P, Striessnig J, Shin HS, Isbrandt D, Ehmke H, Nargeot J, Mangoni ME. Functional roles of ca(v)1.3, ca(v)3.1 and hcn channels in automaticity of mouse atrioventricular cells: Insights into the atrioventricular pacemaker mechanism. Channels (Austin, Tex. 2011; 5:251–261.
36. Gao Z, Rasmussen TP, Li Y, Kutschke W, Koval OM, Wu Y, Hall DD, Joiner ML, Wu XQ, Swaminathan PD, Purohit A, Zimmerman K, Weiss RM, Philipson KD, Song LS, Hund TJ, Anderson ME. Genetic inhibition of na+-ca2+ exchanger current disables fight or flight sinoatrial node activity without affecting resting heart rate. Circ Res. 2013; 112:309–317. [PubMed: 23192947]
37. Sipido KR, Volders PG, Vos MA, Verdonck F. Altered na/ca exchange activity in cardiac hypertrophy and heart failure: A new target for therapy? Cardiovasc Res. 2002; 53:782–805. [PubMed: 11922890]
38. Sipido KR, Volders PG, Schoenmakers M, De Groot SH, Verdonck F, Vos MA. Role of the na/ca exchanger in arrhythmias in compensated hypertrophy. Ann N Y Acad Sci. 2002; 976:438–445. [PubMed: 12502593]
39. Bers DM, Pogwizd SM, Schlotthauer K. Upregulated na/ca exchange is involved in both contractile dysfunction and arrhythmogenesis in heart failure. Basic Res Cardiol. 2002; 97(Suppl 1):I36–42. [PubMed: 12479232]
40. Koster OF, Szigeti GP, Beuckelmann DJ. Characterization of a [ca2+]i-dependent current in human atrial and ventricular cardiomyocytes in the absence of na+ and k+ Cardiovasc Res. 1999; 41:175–187. [PubMed: 10325965]

Novelty and Significance

What Is Known?

- Ion channels and transporters require complex trafficking and retention pathways to modulate cardiac cell excitability.
- In non-cardiac cell-types, endosome pathways play critical roles in membrane protein trafficking, internalization, and recycling.
- Eps15 homology domain (EHD) family gene products were recently identified in heart, associated with membrane protein trafficking in myocytes, and shown to be altered in multiple forms of heart disease.

What New Information Does This Article Contribute?

- Global deficiency of EHD3 in mice results causes in vivo defects in cardiac structure and electrical function including chamber dilation, reduced ejection fraction, bradycardia, and conduction defects.
- EHD3 deficient myocytes display defects in ion channel and transporter expression, membrane localization, and function. These defects are associated with loss of the membrane adapter protein ankyrin-B.
- Mice that selectively lack EHD3 in cardiomyocytes show similar cardiac phenotypes of global EHD3-deficient mice, demonstrating a key role of the EHD3-based endosome pathway in cardiovascular physiology.

Cardiac excitability is governed by the synchronized activities of a host of membrane-bound ion channels, transporters, and receptors. While the field has gained significant insight into the pathways governing membrane protein structure and biophysical function in health and disease, little is known regarding the cellular mechanisms that regulate membrane protein expression, trafficking, and internalization at baseline or in response to acute or chronic stress. As these mechanisms are fundamental for cardiac structural and electrical remodeling in heart failure, new in vivo studies focused on these pathways are essential for generating new therapeutic targets for disease. Our results using new in vivo models demonstrate key roles for the cardiac endosome-based system for membrane protein targeting. Further, these data show that lack of the endosome Eps15 homology domain 3 protein (EHD3) results in both cardiac structural and electrical phenotypes. Together, our findings provide new in vivo data that link endosome-based intracellular protein trafficking pathways with the expression, membrane targeting, and function of key cardiac membrane proteins. As altered EHD3 levels have been previously linked with multiple forms of heart failure, our findings may identify new markers and therapeutic avenues for the diagnosis and treatment of cardiovascular disease.

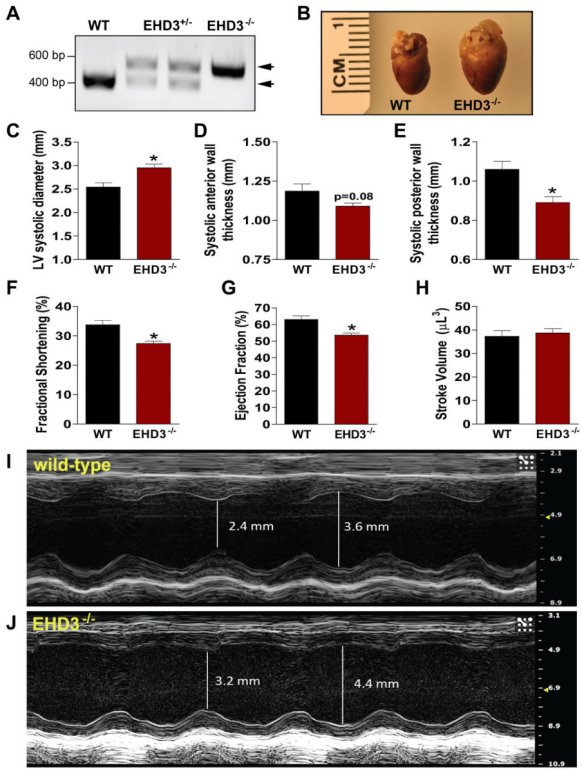

Figure 1. EHD3$^{-/-}$ mice display abnormal cardiac function

(A) Genotyping of WT, EHD3$^{+/-}$, and EHD3$^{-/-}$ mice assessed by PCR of DNA isolated from tail clips of 8-10 day old mice. **(B)** Representative whole hearts isolated from WT and EHD3$^{-/-}$ mice. **(C)** LV systolic diameter is increased in EHD3$^{-/-}$ hearts. **(D)** Systolic anterior wall thickness is increased in EHD3$^{-/-}$ hearts. **(E)** Systolic posterior wall thickness is increased in EHD3$^{-/-}$ hearts. **(F)** Fractional shortening is decreased in EHD3$^{-/-}$ hearts. **(G)** Ejection fraction is decreased in EHD3$^{-/-}$ hearts. **(H)** Stroke volume is preserved across genotypes. **(I-J)** Representative echocardiographic images from WT and EHD3$^{-/-}$ mice; * $p<0.05$, n=7 WT, n=6 EHD3$^{-/-}$.

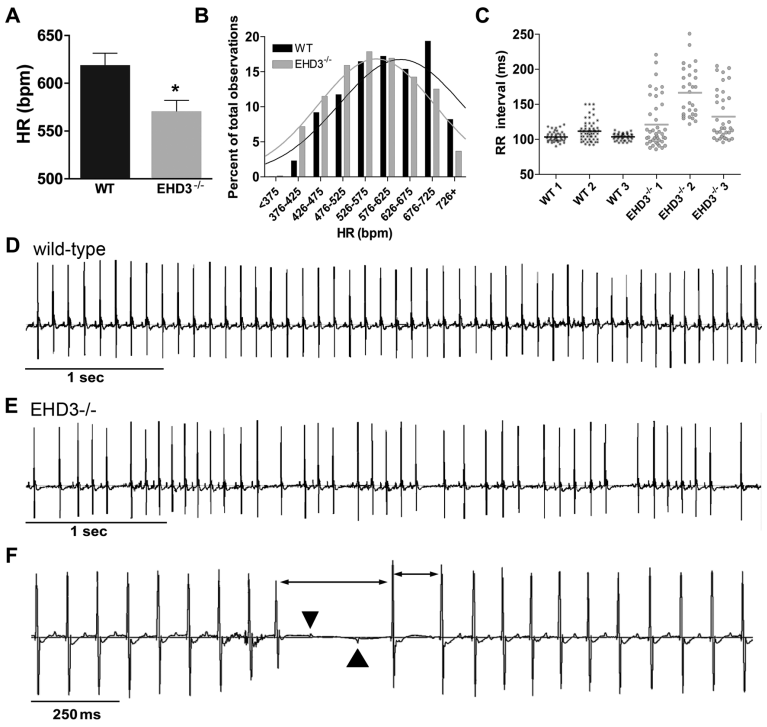

Figure 2. EHD3$^{-/-}$ mice display heart rate variability and conduction defects

(A) EHD3$^{-/-}$ mice display bradycardia compared with WT littermates. **(B)** Distribution of heart rate variability of WT and EHD3$^{-/-}$ mice. In A-B, n=5 for each genotype, $p<0.05$. **(C)** EHD3$^{-/-}$ mice were prone to bursts of irregular R to R interval variability not seen in WT mice. **(D)** Selected five second trace of a WT mouse radiotelemetry demonstrating regular HR. **(E)** Selected five second trace of an EHD3$^{-/-}$ mouse demonstrating a burst of high R to R interval variability. **(F)** Trace of an EHD3$^{-/-}$ mouse demonstrating type II AV conduction block.

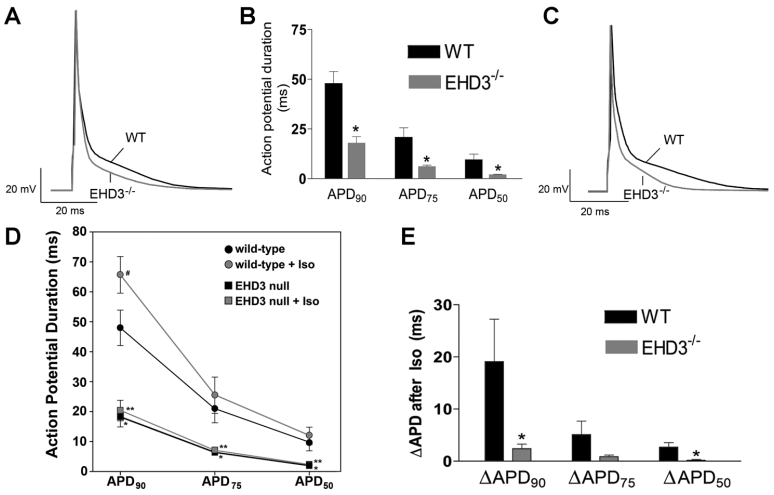

Figure 3. EHD3-deficient myocytes display shortened action potential duration

(A) Representative baseline AP waveform in WT (*black*) and EHD3$^{-/-}$ (*red*) mice. **(B)** APD at baseline. **(C)** Representative AP waveform after application of 100 nM Iso in WT (*black*) and EHD3$^{-/-}$ (*red*) myocytes. **(D)** APD_{90}, APD_{75}, and APD_{50} (± Iso) in WT and EHD3$^{-/-}$ myocytes. **(E)** Change in APD after Iso application. For data in figure, *p<0.05 vs WT, #p<0.05 vs. WT + Iso, n=7 mice/genotype).

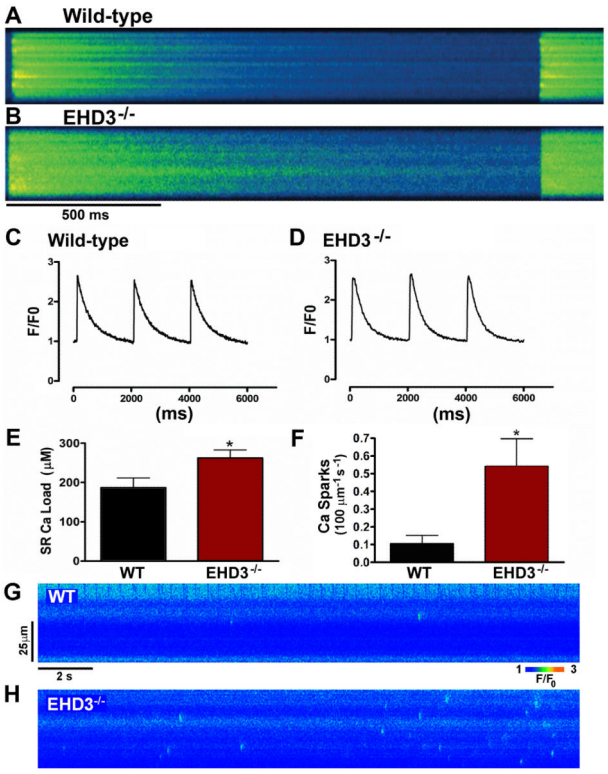

Figure 4. EHD3-deficient myocytes display increased SR Ca load and Ca spark frequency

(A-B) Representative linescan images of 0.5 Hz Ca transients in WT and EHD3$^{-/-}$ myocytes. **(C-D)** Representative Ca transients of WT and EHD3$^{-/-}$ myocytes, normalized to F_0. **(E)** Average SR Ca load in WT (186 ± 25 μM, n = 9) and EHD3$^{-/-}$ (262 ± 20 μM, n = 14) myocytes. **(F)** Spark frequency is increased in EHD3$^{-/-}$ compared to WT myocytes (0.55±0.15 vs. 0.1±0.05 sparks 100 μm^{-1} s^{-1}, n=9 each). Representative confocal linescan images of sparks in WT **(G)** and EHD3$^{-/-}$ **(H)** myocytes.

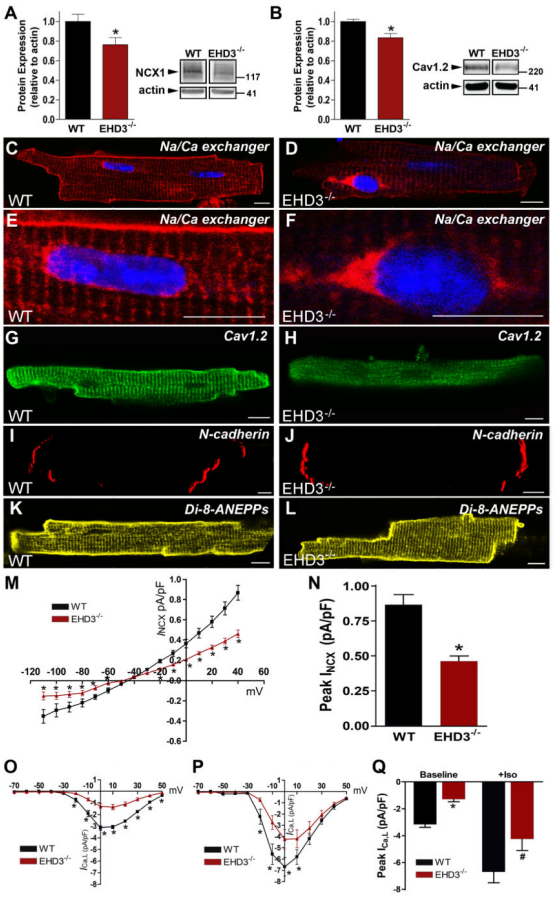

Figure 5. EHD3 regulates NCX and $Ca_V1.2$ membrane targeting and function in heart

(A) NCX expression is decreased by 17% in $EHD3^{-/-}$ hearts (left), representative immunoblot (right). Space between lanes denotes that data were collected from noncontiguous lanes of the same gel. **(B)** $Ca_V1.2$ expression is decreased by 24% in $EHD3^{-/-}$ hearts (left), representative immunoblot (right); n=8 hearts/WT, n=9 hearts/ $EHD3^{-/-}$ for immunoblots (*p<0.05 vs. WT). **(C-L)** Representative confocal images of WT and $EHD3^{-/-}$ isolated ventricular cardiomyocytes displaying localization of Na/Ca exchanger, Cav1.2, N-cadherin, and di-8-ANEPPs (T-tubule marker). Scale bar= 10 microns for all images. **(M-N)** Whole cell I_{NCX} was decreased in $EHD3^{-/-}$ myocytes (n=10 myocytes/genotype). Specifically, peak I_{NCX} was decreased by 47% in $EHD3^{-/-}$ myocytes. **(O-P)** $EHD3^{-/-}$ myocytes display reduced $I_{Ca,L}$ compared to WT at baseline and following 100 nM Iso (n=6 myocytes/genotype, *p<0.05 vs. WT). **(Q)** Peak $I_{Ca,L}$ is significantly decreased in $EHD3^{-/-}$ myocytes ±Iso.

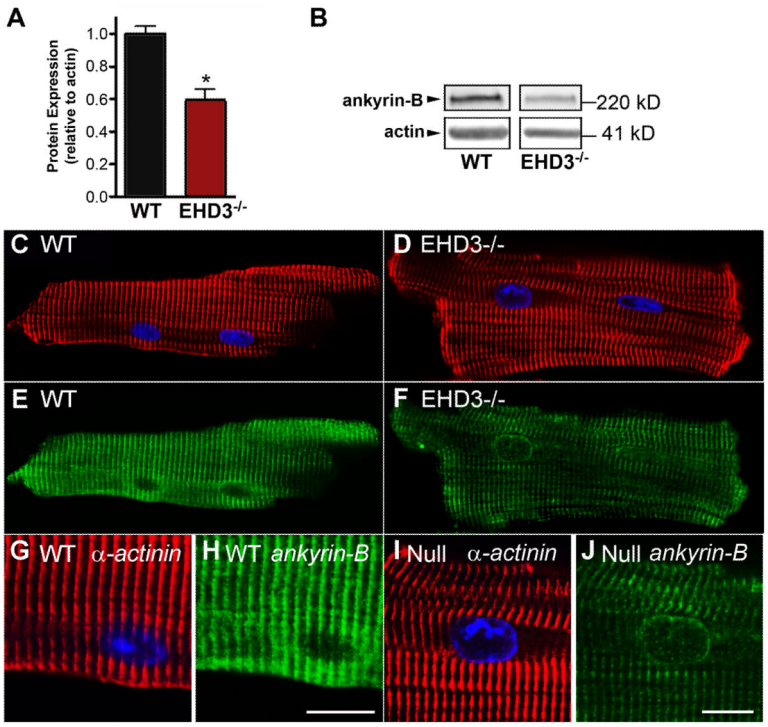

Figure 6. Dysregulation of ankyrin-B expression and localization in EHD3$^{-/-}$ heart

(A) Ankyrin-B expression is reduced ~40% in EHD3$^{-/-}$ hearts (n=9 WT, 8 EHD3$^{-/-}$; *p<0.05 vs. WT). **(B)** Representative immunoblot of ankyrin-B expression in WT and EHD3$^{-/-}$ hearts. Space between lanes denotes that data were collected from noncontiguous lanes of the same gel. **(C-J)** Representative confocal images detailing ankyrin-B trafficking dysregulation in EHD3$^{-/-}$ myocytes; (*p<0.05 vs. WT).

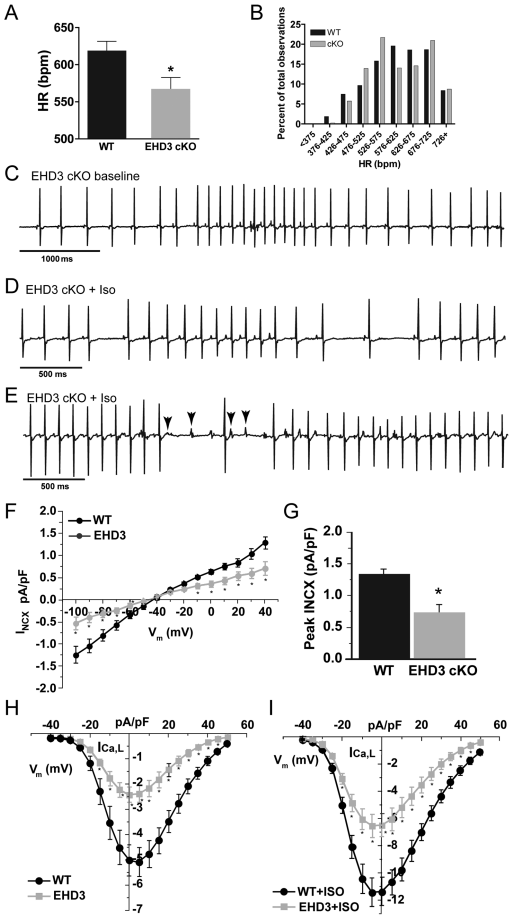

Figure 7. Cardiac-specific EHD3$^{-/-}$ mice phenocopy global EHD3$^{-/-}$ mouse electrical phenotypes

(A) EHD3$^{-/-}$ cKO mice display bradycardia compared with WT littermates. **(B)** Distribution of heart rate variability of WT and EHD3$^{-/-}$ cKO mice. In A-B, n=4 for each genotype, $p<0.05$. **(C)** EHD3$^{-/-}$ cKO mice were prone to bursts of irregular R to R interval variability at baseline not seen in WT mice. **(D)** Selected trace of cKO mouse radiotelemetry demonstrating sinus pause and rate variability following Iso. **(E)** Selected trace of cKO mouse demonstrating AV conduction block phenotypes.